

## Full Length Article

## A GAN-based deep enhancer for quality enhancement of retinal images photographed by a handheld fundus camera

Junxia Fu<sup>a,b,c</sup>, Lvchen Cao<sup>d</sup>, Shihui Wei<sup>c</sup>, Ming Xu<sup>b</sup>, Yali Song<sup>b</sup>, Huiqi Li<sup>e,\*\*</sup>, Yuxia You<sup>a,b,\*</sup><sup>a</sup> Beijing Aier Intech Eye Hospital, Beijing, China<sup>b</sup> Aier Eye Hospital Group, Hunan, China<sup>c</sup> Department of Ophthalmology, The Chinese People's Liberation Army General Hospital, Beijing, China<sup>d</sup> School of Artificial Intelligence, Henan University, Zhengzhou, China<sup>e</sup> School of Information and Electronics, Beijing Institute of Technology, Beijing, China

## ARTICLE INFO

## Keywords:

Generative adversarial networks (GANs)

Retinal image

Quality

Handheld fundus cameras

## ABSTRACT

**Objective:** Due to limited imaging conditions, the quality of fundus images is often unsatisfactory, especially for images photographed by handheld fundus cameras. Here, we have developed an automated method based on combining two mirror-symmetric generative adversarial networks (GANs) for image enhancement.

**Methods:** A total of 1047 retinal images were included. The raw images were enhanced by a GAN-based deep enhancer and another methods based on luminosity and contrast adjustment. All raw images and enhanced images were anonymously assessed and classified into 6 levels of quality classification by three experienced ophthalmologists. The quality classification and quality change of images were compared. In addition, image-detailed reading results for the number of dubiously pathological fundi were also compared.

**Results:** After GAN enhancement, 42.9% of images increased their quality, 37.5% remained stable, and 19.6% decreased. After excluding the images at the highest level (level 0) before enhancement, a large number (75.6%) of images showed an increase in quality classification, and only a minority (9.3%) showed a decrease. The GAN-enhanced method was superior for quality improvement over a luminosity and contrast adjustment method ( $P < 0.001$ ). In terms of image reading results, the consistency rate fluctuated from 86.6% to 95.6%, and for the specific disease subtypes, both discrepancy number and discrepancy rate were less than 15 and 15%, for two ophthalmologists.

**Conclusions:** Learning the style of high-quality retinal images based on the proposed deep enhancer may be an effective way to improve the quality of retinal images photographed by handheld fundus cameras.

## 1. Introduction

Digital retinal imaging is emerging as an important diagnostic tool in the field of ophthalmology, and it can be an indicator of eye or systemic diseases.<sup>1-5</sup> However, the quality of fundus photography is often unsatisfactory due to limited imaging conditions, such as low contrast, insufficient brightness, and uneven illumination, or primary eye diseases, such as media opacity caused by a corneal scar, cataract or vitreous degeneration, myosis, or nystagmus. These problems are particularly prominent in images photographed by handheld devices because of the reduction in hardware size. A hazy retinal structure inevitably increases the difficulty in early detection of microscopic lesions, which may lead to a potential visual impairment and cause socioeconomic burden

worldwide,<sup>6</sup> besides, low contrast further makes it harder to make an accurate computer-aided diagnosis.<sup>7,8</sup> Therefore, it is essential to obtain high-quality retinal images for reliable diagnostic results. A straightforward way is to use a high-performance fundus camera to provide more vivid color and richer details. It is also important to improve the professional skills of photographers. Actually, due to the high cost and paucity of medical resources, it is difficult to popularize the above two means in less developed regions.

With the advent of the fourth industrial revolution, artificial intelligence (AI) has exhibited exponential breakthroughs.<sup>9</sup> Many AI studies have reported promising results for diagnosis and prognosis, and greatly contributed to clinical decision-making. AI-assisted image enhancement aims to improve the visibility of useful information for a raw image

\* Corresponding author. Beijing Aier Intech Eye Hospital, No.12, Panjiayuan Nanli Road, Chaoyang District, Beijing, 100021, China

\*\* Corresponding author. School of Information and Electronics, Beijing Institute of Technology, Beijing, 100081, China.

E-mail addresses: [huiqili@bit.edu.cn](mailto:huiqili@bit.edu.cn) (H. Li), [yoyuxia@hotmail.com](mailto:yoyuxia@hotmail.com) (Y. You).<https://doi.org/10.1016/j.aopr.2022.100077>

Received 28 May 2022; Received in revised form 5 August 2022; Accepted 12 August 2022

Available online 19 August 2022

2667-3762/© 2022 The Authors. Published by Elsevier Inc. on behalf of Zhejiang University Press. This is an open access article under the CC BY-NC-ND license (<http://creativecommons.org/licenses/by-nc-nd/4.0/>).

(usually a quality degraded image), and it could be a distortion process. The specific enhancement goals include targeting to emphasize the overall or local characteristics, sharpen the original unclear portion, intensify certain features of interest, or suppress features that are not related. For retinal images photographed by handheld devices, the main issues are insufficient brightness and low contrast. Thus, improving the overall contrast and brightness is the primary purpose. However, retinal images have their unique morphological characteristics and color, and some standard methods are not applicable for enhancing the retinal images. Generative adversarial networks (GANs) are a set of deep neural network models used to automatically generate synthetic data.<sup>9</sup> Each trained GAN model can be transferred outside of its protected servers to generate different synthetic images from the original, while still preserving disease-relevant imaging features,<sup>9</sup> and GANs have been developed to generate retinal images to improve the classification and diagnosis in the field of ophthalmology.<sup>10-15</sup>

In our work, we have developed an automated method based on combining two mirror-symmetric GANs for retinal image enhancement. By learning the characteristics from a set of high-quality retinal images photographed by a handheld fundus camera, the raw images and enhanced images were independently classified into different levels of quality grading by three ophthalmologists. The statistics of quality changes after enhancement were compared with the enhancement performance of another published method,<sup>16</sup> which is mainly based on the contrast stretching of pixels.

## 2. Methods

### 2.1. Subjects and retinal images

This study was approved by the Beijing Aier Intech Eye Hospital ethics committee. A total of 1047 retinal images from 529 patients were included from October 2018 to November 2018. A consecutive sequence of retinal images was obtained through the Mulin telemedicine platform (Hunan Super Vision Technology Co., Ltd.). The Miis DSC 200 handheld non-mydratic fundus camera was used to capture these retinal images. All retinal images were taken at a 45° angle of view and had a resolution of 2560 × 1920 pixels.

### 2.2. Human vision-based quality grading system

We further extended the existing quality grading standard<sup>17</sup> and devised a more complicated quality grading system to assess the retinal images. The visibility of the optic disk and blood vessels was used as the leading indicator of image quality. We defined the image quality grading system as referred to the grading standard of fundus image of cataract screening and assessment,<sup>18</sup> which was according to the basic theory—the diameter of blood vessels reduced as the vessels branched further, and the optic disk was usually the most apparent retinal structure. Table 1 lists the detailed 6 levels of quality classification with the corresponding typical images shown in Fig. 1.

**Table 1**  
Human vision based image quality grading system.

Grading Category	Description
Level 0	Small vessels after two bifurcations are clearly visible and edges are sharp.
Level 1	Small vessels after two bifurcations are visible while edges are not sharp.
Level 2	Small vessels after two bifurcations are invisible.
Level 3	Only main vessels and optic disk are visible.
Level 4	Only the optic disk is visible.
Level 5	No retinal structure is visible.

As shown in Table 1, the retinal image quality was classified into 6 levels and Figures A to F represent the quality levels from 0 to 5, respectively. In Fig. 1, image A has good quality, in which the optic disk, macula, and blood vessels are visible, and the edges of small vessels are sharp. The quality of image B is less than that of image A, but the small vessels are still visible. The main vessels are visible in image C, while the small vessels after two bifurcations are invisible. The optic disk is visible in image D, and the main vessels are faintly visible. In image E, only the optic disk is visible. Almost no retinal structures can be observed in image F. In total, the higher the image quality, the more visible the retinal structures.

### 2.3. Image enhancement method

We have previously developed the deep enhancer,<sup>19</sup> and it aimed to improve the overall quality of retinal images through learning the characteristics from a set of high-quality images, and Fig. 2 illustrates its framework.

The goal of the deep enhancer was to train mapping functions between two data sets. In the training process, the images in the two training sets need not be paired one by one, and the two data sets should have different characteristics. As shown in Fig. 2, this model included two mapping functions, and they constantly generated intermediate results during the training process. The retinal images of data set 2 had higher contrast and brightness compared to the retinal images of data set 1. The two discriminators were used to distinguish the style differences between the intermediate results and target images. Through back-propagation of neural network parameters, the two generators' learning ability became more substantial, along with a reduction in the loss function associated with image style.<sup>19</sup> The training stopped when the two discriminators could not judge the style difference between the intermediate results and the target images.

After the style transfer by the trained deep enhancer, the retinal images in data set 1 obtained the style of retinal images in data set 2. Both the contrast level and brightness level of data set 1 were improved and were similar to those of data set 2. Thus, the goal of improving the image quality was achieved. In this test, the two sets of retinal images were photographed by different fundus cameras. Data set 1 was acquired by using a handheld fundus camera (Miis DSC200), and data set 2 was acquired by using a relatively high-end fundus camera (Canon CR-2). Accordingly, the outputs of mapping function 1 were the enhancement results, and three ophthalmologists assessed them based on the quality grading system.

### 2.4. Single-blind assessment

Three ophthalmologists (S, Y, and Z) assessed the raw images and the corresponding enhanced images. The specific process was as follows: firstly, based on the quality grading system, the 1047 raw images were classified into six levels; secondly, these 1047 images were enhanced by our proposed deep enhancer and another image enhancement method<sup>16</sup>; and then the order of the enhanced images was randomly shuffled for further assessment. Once again, quality assessment of enhanced images was performed by the three ophthalmologists. The assessment results of raw and enhanced images were independently recorded.

In addition to the single-blind results, we also voted on the assessment results. As quality degradation is a gradual process, it is difficult to accurately determine the quality grading. Besides, different subjective judgments may affect the assessment results. For the sake of fairness, we determined the quality of each image based on majority voting. When two or more ophthalmologists had the same assessment results, the quality of a retinal image was determined. When all assessments of the three ophthalmologists were different, we used the intermediate value as the final decision.

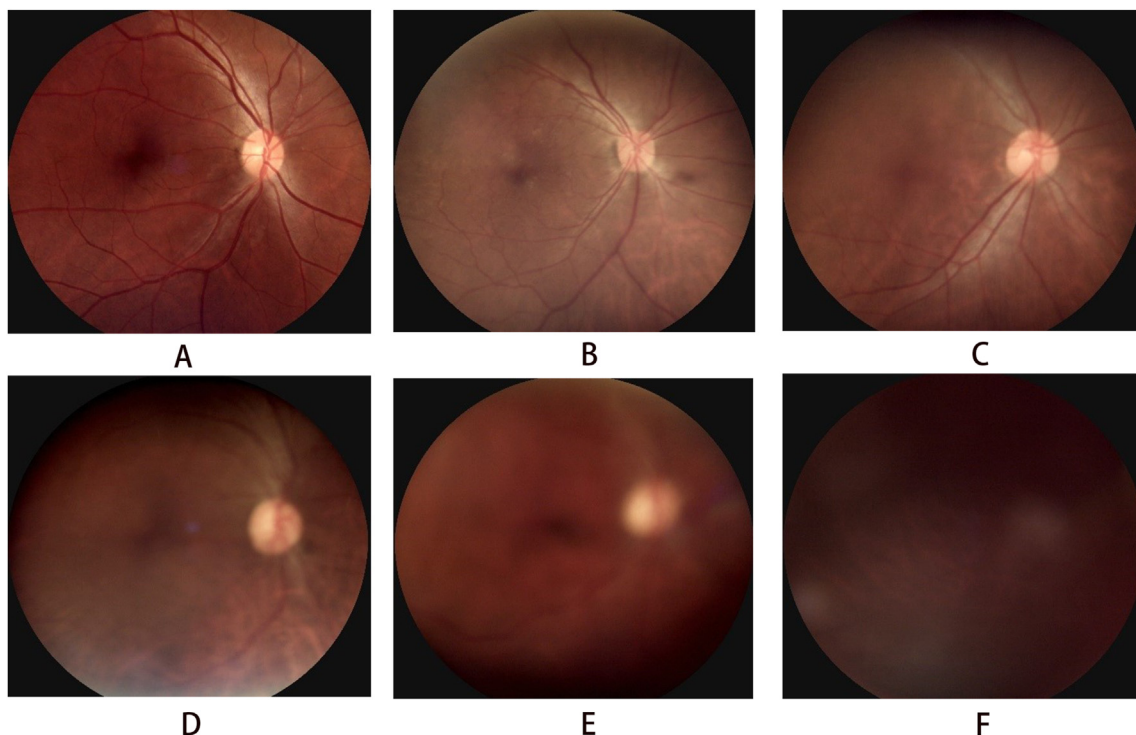


Fig. 1. Quality classifications of retinal images. A-F denoted the 6 levels from 0 to 5.

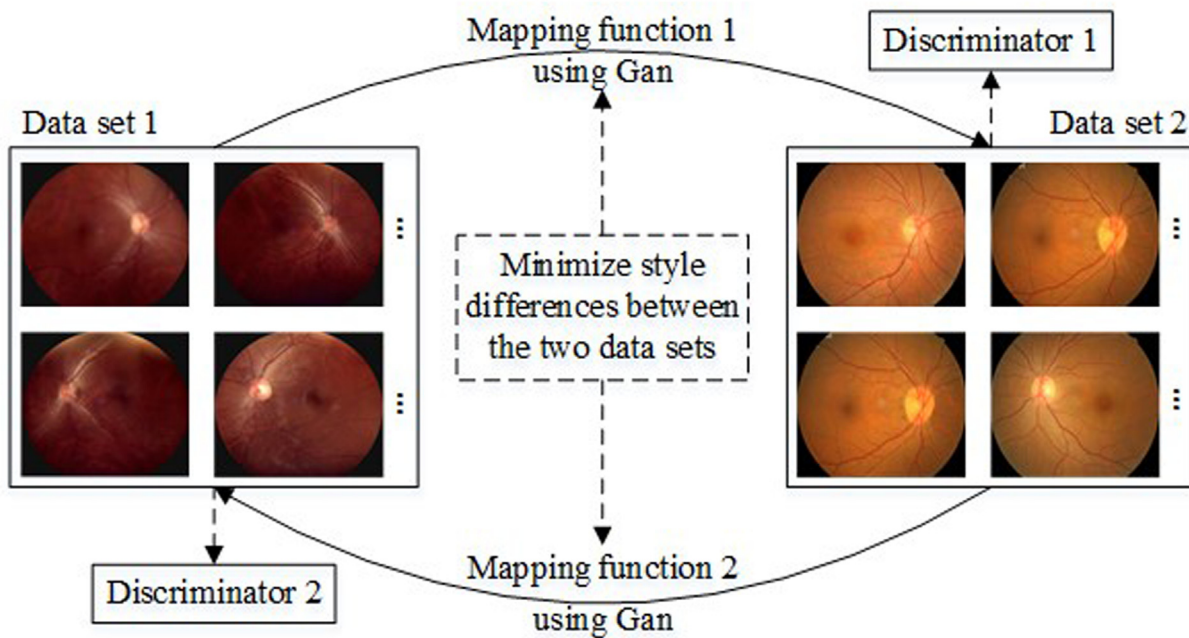


Fig. 2. The framework of the deep enhancer for the retinal image.

2.5. Comparison of the image reading results before and after GAN enhancement

In order to accurately evaluate the effects of enhanced images on doctors' judgment, we divided fundus images into a roughly normal fundus and dubiously pathological fundus, and the latter was further divided into the following 8 types: diabetic retinopathy, glaucoma, maculopathy, hemorrhage due to other diseases, high myopic retinopathy, hypertensive retinopathy, optic neuropathy, and unreadable

pictures. We recorded the number of reading results for each ophthalmologist before and after image enhancement, independently, and counted the number of consistent reading results between each other before and after image enhancement. The consistency rate for pre- and post-enhancement was calculated by the smaller number divided by the larger number. For the subtypes whose number was more than 30 before and after enhancement, we calculated the discrepancy rate, which was equal to the discrepancy number divided by the larger number of pre- or post-enhancement.

### 3. Results

#### 3.1. Distribution of quality assessments and quality changes for images after enhancement

The number of completely consistent quality grading results between three ophthalmologists were 731 (69.82%) for raw data, 723 (69.05%) for GAN-enhanced data, and 721 (68.86%) for color retinal image enhanced data, respectively. For the quality ratings inconsistent pictures, two ophthalmologists had consistent grading results, and the remaining ophthalmologist scored one grade higher or lower than the other two ophthalmologists. None of the picture quality score results varied by more than one grade. The assessment results for the three ophthalmologists and major voting before and after retinal image enhancement were shown in Table 2 and the detail information was shown in Supplement Table 1 to 8. A significantly increasing trend in the number distribution of assessments was observed after the two image enhancements, and 65.2% and 48.6% of the images reached up to level 0 in terms of image quality, and 245 (23.4%) and 379 (36.2%) reached up to level 1, respectively ( $P < 0.001$ , Table 2). Detailed information about quality changes is shown in Table 3 and Supplement Table 9. As shown in Supplement Figure 1, Figure A and B increased quality, Figure C and D maintained stable quality, whereas Figure E reduced quality after GAN enhancement. Although quality level 0 and level 1 occupied a large proportion after enhancement, 19.6% (205/1047) and 26.9% (282/1047) of the images still showed a decrease in quality after GAN-based deep enhancement and luminosity and contrast adjustment, respectively (Supplement Table 9). However, approximately one-third of the images; 393 (37.5%) images after GAN-based deep enhancement and 401 (38.3%) images after image enhancement based on luminosity and contrast adjustment showed no change in the quality grade after enhancement (Supplement Table 9).

#### 3.2. Detailed quality assessments excluded images at level 0 before enhancement

We performed a further analysis of the detailed change for retinal images which were not changed after enhancement. As demonstrated in Table 4, more than half of the retinal images, 66.4% and 53.1%, respectively, were at level 0 before quality processing. Thus, in order to veritably evaluate the effect of image enhancement, we excluded the 597 (57%) images at level 0 individually or by vote before enhancement, and finally, 450 images were included in our analysis. Table 5 showed that a large number of retinal images photographed by a handheld fundus camera were increased after enhancement, 340 (75.6%) and 287 (63.8%), respectively, whereas, merely a minority of images decreased after image processing (9.3% and 11.3%, respectively). On comparing

the two image processing methods, the GAN-enhanced method obtained a better advantage for image improvement ( $P < 0.001$ ). Specifically, a large number of retinal images, 46.9% and 39.8%, respectively, increased one level after enhancement (Table 5). Among them, the images that changed from level 1 to level 0 dominated a majority (82.5% and 69.8%, respectively, Supplement Table 10). Of the 22 images that decreased one level after GAN-image processing, 15 images changed from level 1 to level 2, six images changed from level 2 to level 3, and only one image changed from level 3 to level 4 (Supplement Table 11).

#### 3.3. Comparison of image reading results before and after GAN enhancement

As shown in Table 6, although the number of abnormal lesions decreased slightly after GAN enhancement, except for the ophthalmologist Z's results, totally, the consistency rate pre- and post-enhancement fluctuated from 86.6% to 95.6%. In terms of specific disease subtypes, the ophthalmologist Z's diagnosis results showed great fluctuation mainly focused on less unreadable images, more maculopathy, and more high myopia after enhancement; and for the preliminary results of ophthalmologists S and Y, both the discrepancy number and discrepancy rate were less than 15 and 15%, respectively (Table 6 and Fig. 3).

### 4. Discussion

Our study introduced a deep learning technique to improve the quality of retinal images photographed by a handheld fundus camera, without any significantly increased inconsistencies, which may improve the readability and could be widely used for the screening of ophthalmic diseases in community hospitals. Although the GAN system has been previously published and used in the image synthesis task, we have further attempted to apply a pair of GANs to enhance fundus images taken by a handheld device via the domain transformation from a handheld device to a relatively high-end device.

As traditional ophthalmic equipment, a fundus camera, classified into the following two types: tabletop and handheld, is helpful for the diagnosis and early screening of ocular fundus pathology. Actually, due to the high costs and technical difficulty, not all community healthcare centers and remote areas are equipped with table fundus cameras. Due to its features, such as being small, portable, and relatively inexpensive, a hand-held fundus camera is more suitable for disease screening in the crowd. However, due to insufficient brightness and low contrast, the clarity of images photographed by a handheld fundus camera is not always satisfactory. Therefore, image enhancement is a feasible solution for making the acquired images meet the clinical requirements. Retinal image enhancement can improve the quality of retinal images collected in community healthcare centers or ophthalmology clinics, which is the

**Table 2**  
The distribution of quality assessments for retinal images before and after enhancement.

Ophthalmologist	Retinal image	Quality grading (n, %)						P
		Level 0	Level 1	Level 2	Level 3	Level 4	Level 5	
1	Raw data	435 (41.5%)	386 (36.9%)	121 (11.6%)	66 (6.3%)	37 (3.5%)	2 (0.2%)	
	GAN-enhanced data	819 (78.9%)	132 (12.6%)	37 (3.5%)	31 (3.0%)	22 (2.1%)	6 (0.6%)	< 0.001
	Color retinal image enhanced data	368 (35.1%)	475 (45.4%)	129 (12.3%)	50 (4.8%)	24 (2.3%)	1 (0.1%)	< 0.001
2	Raw data	410 (39.2%)	479 (45.7%)	102 (9.7%)	40 (3.8%)	14 (1.3%)	2 (0.2%)	
	GAN-enhanced data	611 (58.4%)	319 (30.5%)	64 (6.1%)	35 (3.3%)	16 (1.5%)	2 (0.2%)	< 0.001
	Color retinal image enhanced data	484 (46.2%)	390 (37.2%)	124 (11.8%)	46 (4.4%)	3 (0.3%)	0	< 0.001
3	Raw data	473 (45.2%)	352 (33.6%)	178 (17.0%)	31 (3.0%)	12 (1.1%)	1 (0.1%)	
	GAN-enhanced data	577 (55.1%)	258 (24.6%)	106 (10.1%)	56 (5.3%)	29 (2.8%)	21 (2.0%)	< 0.001
	Color retinal image enhanced data	675 (64.5%)	243 (23.2%)	83 (7.9%)	40 (3.8%)	5 (0.5%)	1 (0.1%)	< 0.001
Majority voting	Raw data	435 (41.5%)	421 (40.2%)	136 (13.0%)	38 (3.6%)	15 (1.4%)	2 (0.2%)	
	GAN-enhanced data	683 (65.2%)	245 (23.4%)	59 (5.6%)	34 (3.2%)	20 (1.9%)	6 (0.6%)	< 0.001
	Color retinal image enhanced data	509 (48.6%)	379 (36.2%)	110 (10.5%)	43 (4.1%)	5 (0.5%)	1 (0.1%)	< 0.001

Abbreviations: GAN = generative adversarial network.

P–P value for comparison between raw data and enhanced data, including GAN-enhanced data or color retinal image enhanced data.

**Table 3**  
The detailed distribution of quality changes for retinal images before and after enhancement.

Ophthalmologist	Retinal image	Quality changes (n)										
		-5	-4	-3	-2	-1	0	1	2	3	4	5
1	GAN-enhanced data	3	9	19	35	70	399	326	99	59	26	2
	Color retinal image enhanced data	0	6	31	76	245	362	200	81	32	14	0
2	GAN-enhanced data	1	5	23	39	158	393	325	72	22	7	2
	Color retinal image enhanced data	0	0	19	62	219	389	271	59	21	6	1
3	GAN-enhanced data	10	19	39	72	165	359	250	110	16	6	1
	Color retinal image enhanced data	0	2	20	50	146	408	267	123	24	6	1
Majority voting	GAN-enhanced data	3	8	25	38	131	393	316	99	21	11	2
	Color retinal image enhanced data	0	2	18	66	196	401	253	82	20	8	1

Abbreviations: GAN = generative adversarial network.

A positive number represented an increase in image quality changes after enhancement, a negative number represented a reduction in image quality changes after enhancement, and zero represented no change in image quality changes after enhancement.

**Table 4**  
The distribution of quality changes for retinal images which was not changed after enhancement.

Ophthalmologist	Retinal image	Quality Change (n, %)						Total
		0 to 0	1 to 1	2 to 2	3 to 3	4 to 4	5 to 5	
1	GAN-enhanced data	338 (84.7%)	50 (12.5%)	6 (1.5%)	4 (1%)	1 (0.3%)	0	399
	Color retinal image enhanced data	158 (43.6%)	185 (51.1%)	16 (4.4%)	3(0.8%)	0	0	362
2	GAN-enhanced data	247 (62.8%)	140 (35.6%)	4 (1.0%)	2 (0.5%)	0	0	393
	Color retinal image enhanced data	205 (52.7%)	173 (44.5%)	10 (2.6%)	1 (0.3%)	0	0	389
3	GAN-enhanced data	255 (71.0%)	85 (23.7%)	18 (5%)	1 (0.3%)	0	0	359
	Color retinal image enhanced data	310 (76%)	84 (20.6%)	13 (3.2%)	1 (0.2%)	0	0	408
Majority voting	GAN-enhanced data	261 (66.4%)	116 (29.5%)	13 (3.3%)	1 (0.3%)	2 (0.5%)	0	393
	Color retinal image enhanced data	213 (53.1%)	161 (40.1%)	20 (5%)	5 (1.2%)	2 (0.5%)	0	401

**Table 5**  
The distribution of quality changes for retinal images after excluded images level 0 before enhancement.

Retinal image		GAN-enhanced data	Color retinal image enhanced data	P
Quality changes (n, %)	increase	340 (75.6%)	287 (63.8%)	< 0.001
	unchanged	68 (15.1%)	112 (24.9%)	
	decrease	42 (9.3%)	51 (11.3%)	
Quality changes in detail (n, %)	-4	1 (0.2%)	0	
	-3	10 (2.2%)	2 (0.4%)	
	-2	9 (2.0%)	16 (3.6%)	
	-1	22 (4.9%)	33 (7.3%)	
	0	68 (15.1%)	112 (24.9%)	
	1	211 (46.9%)	179 (39.8%)	
	2	95 (21.1%)	79 (17.6%)	
	3	21 (4.7%)	20 (4.4%)	
	4	11 (2.4%)	8 (1.8%)	
	5	2 (0.4%)	1 (0.2%)	

Abbreviations: GAN = generative adversarial network.

A positive number represented an increase in image quality changes after enhancement, a negative number represented a reduction in image quality changes after enhancement, and zero represented no change in image quality changes after enhancement.

guarantee for clinical diagnosis and further artificial intelligence analysis. From the perspective of the government, it helps to save medical resources and reduce health care costs.

However, retinal image has their unique morphological characteristics and color, and some standard methods may not be applicable for enhancing the retinal images.<sup>20</sup> For example, the retina cortex-based method performs well in outdoor image enhancement, while over enhancement produces heavy noise when applied to retinal images. Zhou et al. proposed a reliable enhancement method for the retinal images,<sup>16</sup> which consisted of brightness and contrast improvement. The first step is to improve the visibility of retinal structures in dark areas by using a Gamma map. Based on the contrast limited adaptive histogram equalization, the contrast improvement can easily introduce the apparent

noise. Enhancement using a matched filter is beneficial for improving the contrast of blood vessels,<sup>21-23</sup> but it hurts the other retinal structures. Xiong et al. proposed an enhancement method for retinal images based on a scattering model.<sup>24</sup> By appropriately estimating the global atmospheric light and transmission coefficients for each pixel, the method can effectively improve the contrast and preserve the original color.

In our study, 42.9% of primary images achieved an increased quality classification after enhancement, 37.5% did not change, and 19.6% showed decreased quality classification (Supplement Table 9). Thus, a considerable part of the quality grading was not changed mainly because 66.4% of unchanged images were rated at the highest level 0 before enhancement (Table 4). After removing this portion, 75.6% of the original images increased their quality grades, and only 15.1% of images did not change the grading after enhancement (Table 5). It may indicate that the enhancement itself cannot recover the texture information of small vessels that disappear entirely in a raw image. Moreover, 9.3% of images showed a grading decline after enhancement (Table 5); of them, 82.5% decreased from level 1 to level 0 (Supplement Table 10). The possible reasons were as follows: the deep enhancer did not transfer the style very well on the details, or the ophthalmologists may have made some subjective errors when the difference between the two adjacent quality gradings was slight.

We observed that the enhancement method proposed in the previous article, which was based on luminosity and contrast adjustment, was less sensitive to improving the quality of retinal images than our deep enhancer since more images were unchanged or decreased after enhancement ( $P < 0.001$ , Table 5).<sup>16</sup> The number of images with an increase in the quality was less than that in the assessment results based on the deep enhancer ( $P < 0.001$ , Table 5). Thus, our proposed deep enhancer may have a better ability to improve the visual quality of retinal images photographed by a handheld fundus camera compared to the method of color retinal image enhancement.

A good visual effect is the guarantee of a successful diagnosis. Compared to the method of color retinal image enhancement, two sets of typical enhanced images were displayed to show their performance difference. In Fig. 4, the first column A was the raw image, and the second B

**Table 6**  
Comparison of images reading results before and after GAN-enhancement.

Type	Unreadable	Diabetic retinopathy	Glaucoma	Maculopathy	Hemorrhage due to other retinopathy	High myopia retinopathy	Hypertensive retinopathy	Optic neuropathy	Total	Consistency rate
Pre-S	49	32	11	63	11	16	1	0	183	95.6%
After-S	46	34	4	63	14	13	1	0	175	
Discrepancy-S	3	2	7	0	3	3	0	0	8	
Discrepancy rate-S	6.1%	5.9%	-	0	-	-	-	-	4.4%	
Pre-Y	60	38	9	92	17	16	1	0	233	90.1%
After-Y	66	29	4	79	9	19	4	0	210	
Discrepancy-Y	6	9	5	13	8	3	3	0	23	
Discrepancy rate-Y	9.1%	-	-	14.1%	-	-	-	-	9.8%	
Pre-Z	77	12	10	185	14	62	2	5	367	87.2%
After-Z	50	15	8	221	26	97	1	3	421	
Discrepancy-Z	27	3	2	36	12	35	1	2	54	
Discrepancy rate-Z	35.1%	-	-	16.3%	-	36.1%	-	-	12.8%	
Consistency-pre SY	41	25	6	51	9	9	1	0	142	89.4%
Consistency-after SY	39	21	3	50	5	8	1	0	127	
Discrepancy-SY	2	4	3	1	4	1	0	0	15	
Discrepancy rate-SY	4.9%	-	-	2.0%	-	-	-	-	10.6%	
Consistency-pre SZ	39	12	6	58	7	12	0	0	134	91.8%
Consistency-after SZ	32	14	3	57	7	10	0	0	123	
Discrepancy-SZ	7	2	3	1	0	2	0	0	11	
Discrepancy rate-SZ	17.9%	-	-	1.7%	-	-	-	-	8.2%	
Consistency-pre YZ	46	12	8	74	8	12	0	0	160	86.6%
Consistency-after YZ	36	15	3	64	4	15	0	0	137	
Discrepancy-YZ	10	3	5	10	4	3	0	0	23	
Discrepancy rate-YZ	21.7%	-	-	13.5%	-	-	-	-	14.4%	

Pre/After-S: The number of reading results for ophthalmologist S before/After image enhancement.

Pre/After-Y: The number of reading results for ophthalmologist Y before/After image enhancement.

Pre/After-Z: The number of reading results for ophthalmologist Z before/After image enhancement.

Consistency-pre/after SY: The number of consistent reading results between ophthalmologist S and ophthalmologist Y before/after image enhancement.

Consistency-pre/after SZ: The number of consistent reading results between ophthalmologist S and ophthalmologist Z before/after image enhancement.

Consistency-pre/after YZ: The number of consistent reading results between ophthalmologist Y and ophthalmologist Z before/after image enhancement.

and third C columns were the enhancement results based on luminosity and contrast adjustment and GAN deep enhancer, respectively. The contrast can be improved by either method; however, the method based on luminosity and contrast adjustment dramatically enlarges the noise. The enhanced noise may affect the visibility of abnormalities, such as microaneurysm or drusen, since both lesions are tiny. With respect to the enhancement results, GAN enhancement showed better visibility of the main retinal structures, such as the optic disk, blood vessels, and macula, and it could better suppress the noise.

To be more specific, we analyzed the quality improvement in local areas, including the blood vessels, optic disk, and macula (Fig. 5). The three columns represented the image patches from the raw images A, enhanced images based on luminosity and contrast adjustment B, and GAN deep enhancer C, respectively. Generally, the contrast was improved after the former method but it introduced over enhancement as well. For image patch 1, the blood vessels in the enhanced image B lost the primary color and became very dark, which looked like an abnormality. As for the result of the proposed deep enhancer C, although the color style of the retinal background was changed, the vessels' color was preserved. For the optic disk in patch 2, the color of blood vessels in the

optic disk was also distorted in patch B2, and the peripapillary atrophy outside the optic disc should not be black. For the macula in patch 3, over enhancement was also evident after enhancement in patch B3, which may increase the risk of misdiagnosis.

Apart from improving the visual effect of retinal images, the deep enhancer could also help to improve the reliability of automatic retinal image processing. Vessel tracking was employed to demonstrate this improvement.<sup>25</sup> We can use vessel tracking based on the intensity difference between blood vessels and surrounding pixels to measure the parameters of blood vessels, such as the curvature and width. However, quality degraded images often suffer from low contrast, and then the tracking accuracy is easily affected. By using our method to track the blood vessels in the original image and enhanced image, as shown in Fig. 6, it is not difficult to determine that the enhanced image is more conducive to tracking and obtaining the correct blood vessel.

Moreover, our proposed deep enhancer can be easily generalized because the training sets are unpaired and it is convenient to collect image sets with different characteristics. For example, we can achieve the enhancement of blurry retinal images with relatively clear fundus images for cataract patients via a deep enhancer that can deblur after training by

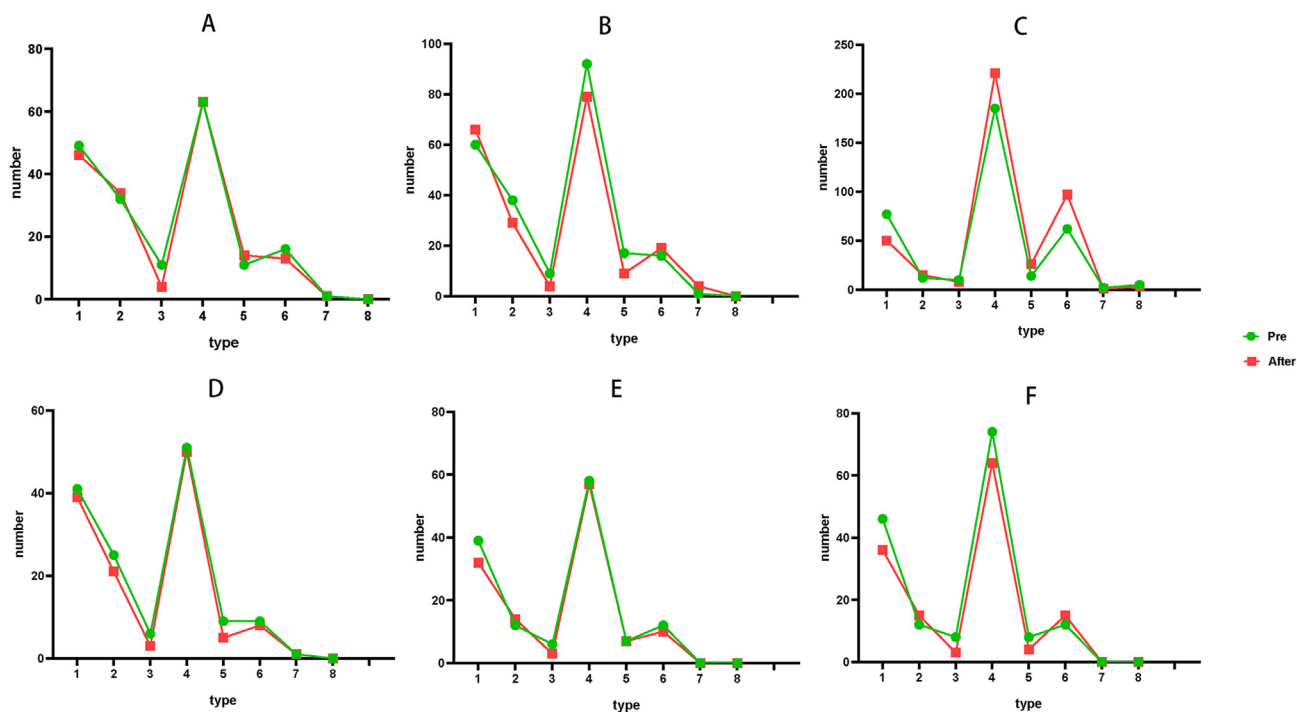


**Fig. 3.** The comparison of the number of retinal image judgment results before and after GAN-enhancement. A–C represented the number of assessment results for ophthalmologists S, Y, and Z, respectively. D–F represented the number of consistent results for the two ophthalmologists—S and Y, S and Z, and Y and Z, respectively. The green line represented the assessment results pre-enhancement, and the red line represented the assessment results after enhancement. GAN: generative adversarial network.

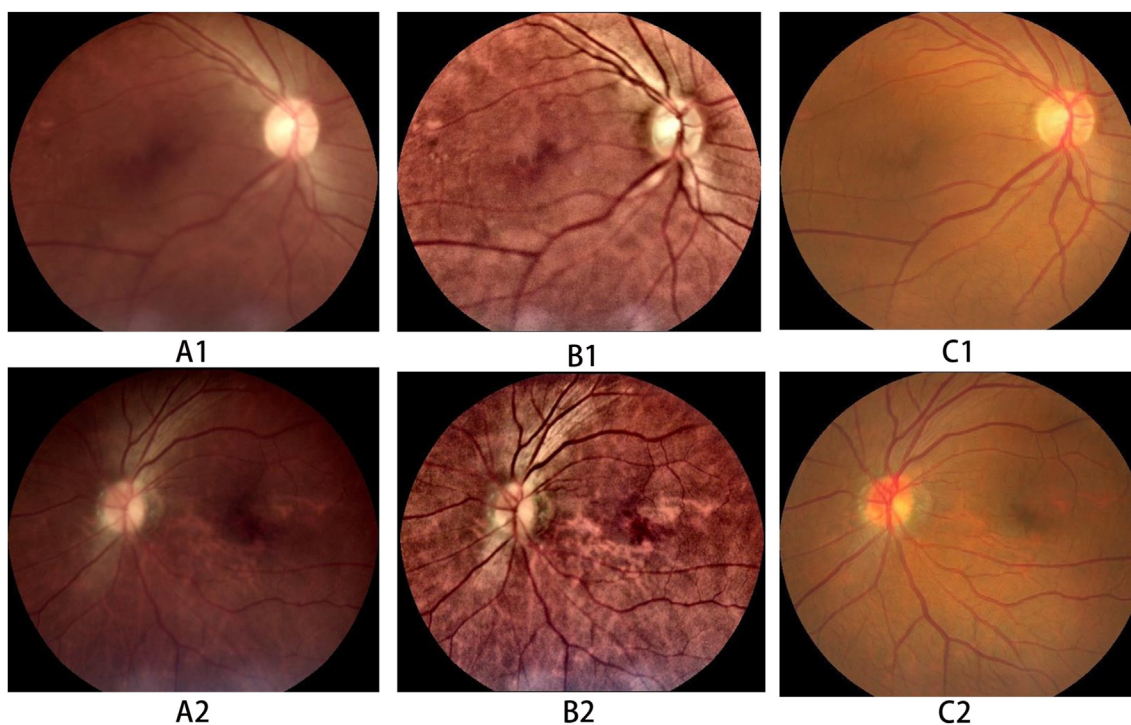


**Fig. 4.** Visual assessment of the retinal images before and after two image enhancements. A. Raw images. B. Retinal images after luminosity and contrast adjustment. C. Retinal images after GAN-based deep enhancer. 1: Fundus photograph of the right eye; 2: Fundus photograph of the left eye. GAN: generative adversarial network.

replacing data set 1 (refer to Fig. 2) with the blurry retinal images from cataract patients.

Our study was the first attempt for the GAN model in retinal images photographed by a handheld fundus camera. It truly has several

limitations. Firstly, the study had a relatively small sample size, and there were a small number of images that did not change their quality classification or showed a decline in quality classification after enhancement. Thus, a large sample is needed to expand and validate our results. In

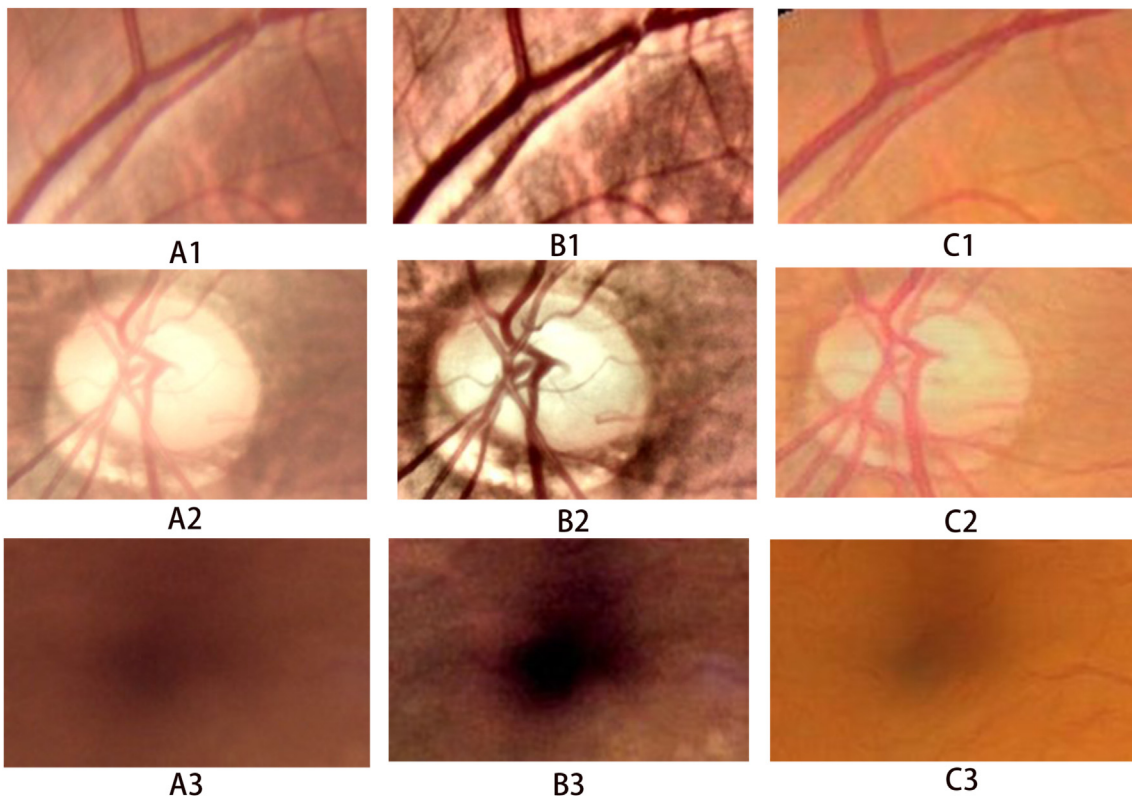


**Fig. 5.** Visual assessment of blood vessels, optic disk, and macula. A. Image patches from raw images; B. Image patches from the enhanced images after luminosity and contrast adjustment; C. Image patches from retinal images after GAN-based deep enhancer. 1: blood vessel; 2: optic disk; 3: macula. GAN: generative adversarial network.

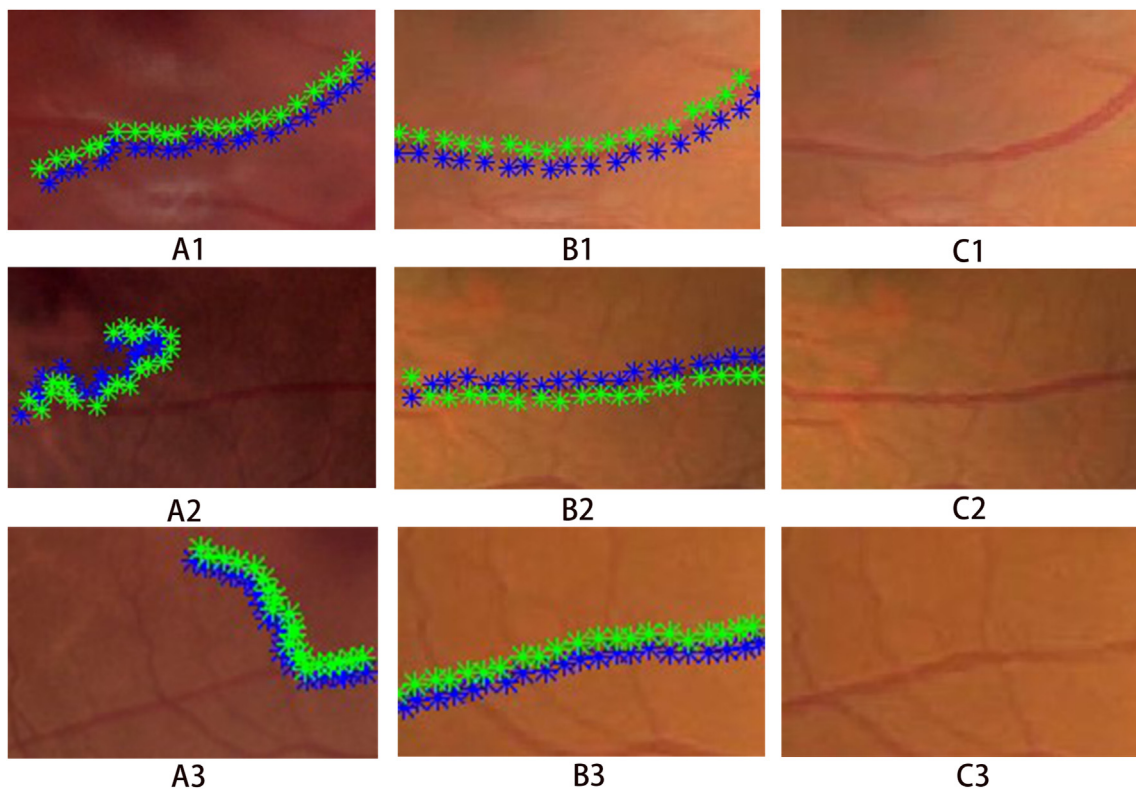


**Fig. 6.** Results of vessel tracking based on the raw images and enhanced images. A. Tracking results using raw images; B. Tracking results using GAN-based enhanced images; C. The image vessel using GAN-based enhancer. The arrows indicate the direction in which the blood vessels are tracking. Successive asterisks represent the trajectory of blood vessel tracking.

addition, because it is a routine screening in the population, we did not have a gold standard for disease diagnosis; therefore, we could not verify the effectiveness of the GAN model in diagnosing specific diseases. Lastly, the limitations of GAN-based enhancement method truly can not be neglected. The information fidelity of dark areas in the original image will decrease in the generated image after enhancement, and this is because the primary purpose of GAN is domain transformation, and small information degradation is easy to occur in the process of domain transformation process. And the training of the GAN model is time-consuming, which decreases the efficiency of parameter tuning.

In general, the quality of handheld fundus photographs could be effectively improved after deep enhancement, which may partially solve the current clinical dilemma. Moreover, the application of the GAN-based deep enhancer in retinal images undoubtedly improves the working efficiency and meets the need for disease-related general investigation in community hospitals without significantly increasing the rate of misdiagnosis.

### Study approval

The study protocol was in accordance with the tenets of the Helsinki Declaration and the ICH-GCP guidelines.

### Author contributions

Conceptualization: HL, YY; Methodology: JF, LC, SW; Formal analysis and investigation: JF, LC; Writing - original draft preparation: JF, LC, YY; Writing - review and editing: JF; Data collection and curation: LC, MX, YS, HL, YY; Supervision: YY.

### Acknowledgments

Thanks to all the peer reviewers for their opinions and suggestions.

### Funding

This research did not receive any specific grant from funding agencies in the public, commercial, or not-for-profit sectors.

### Declaration of competing interest

The authors declare that they have no known competing financial interests or personal relationships that could have appeared to influence the work reported in this paper.

### Appendix A. Supplementary data

Supplementary data to this article can be found online at <https://doi.org/10.1016/j.aopr.2022.100077>.

### References

1. Abramoff MD, Garvin MK, Sonka M. Retinal imaging and image analysis. *IEEE Rev Biomed Eng.* 2010;3:169–208. <https://doi.org/10.1109/rbme.2010.2084567>.
2. Kandasamy Y, Smith R, Wright I, et al. Use of digital retinal imaging in screening for retinopathy of prematurity. *J Paediatr Child Health.* 2013;49:E1–E5. <https://doi.org/10.1111/j.1440-1754.2012.02557.x>.
3. Kankanahalli S, Burlina PM, Wolfson Y, et al. Automated classification of severity of age-related macular degeneration from fundus photographs. *Invest Ophthalmol Vis Sci.* 2013;54:1789–1796. <https://doi.org/10.1167/iovs.12-10928>.
4. Coyner AS, Chen J, Campbell JP, et al. Diagnosability of synthetic retinal fundus images for plus disease detection in retinopathy of prematurity. *AMIA Annu Symp Proc.* 2020;undefined:329–337.
5. Diaz-Pinto A, Colomer A, Naranjo V, et al. Retinal image synthesis and semi-supervised learning for glaucoma assessment. *IEEE Trans Med Imag.* 2019;38:2211–2218. <https://doi.org/10.1109/tmi.2019.2903434>.
6. Wang W, Yan W, Müller A, et al. Association of socioeconomic with prevalence of visual impairment and blindness. *JAMA Ophthalmol.* 2017;135:1295–1302. <https://doi.org/10.1001/jamaophthalmol.2017.3449>.
7. Şevik U, Köse C, Berber T, et al. Identification of suitable fundus images using automated quality assessment methods. *J Biomed Opt.* 2014;19, 046006. <https://doi.org/10.1117/1.Jbo.19.4.046006>.
8. Mookiah MR, Acharya UR, Chua CK, et al. Computer-aided diagnosis of diabetic retinopathy: a review. *Comput Biol Med.* 2013;43:2136–2155. <https://doi.org/10.1016/j.compbiomed.2013.10.007>.
9. Lim JS, Hong M, Lam WST, et al. Novel technical and privacy-preserving technology for artificial intelligence in ophthalmology. *Curr Opin Ophthalmol.* 2022. <https://doi.org/10.1097/icu.0000000000000846>.
10. Pham QTM, Ahn S, Shin J, et al. Generating future fundus images for early age-related macular degeneration based on generative adversarial networks. *Comput Methods Progr Biomed.* 2022;216, 106648. <https://doi.org/10.1016/j.cmpb.2022.106648>.
11. Zheng C, Koh V, Bian F, et al. Semi-supervised generative adversarial networks for closed-angle detection on anterior segment optical coherence tomography images: an empirical study with a small training dataset. *Ann Transl Med.* 2021;9:1073. <https://doi.org/10.21037/atm-20-7436>.
12. Zheng C, Bian F, Li L, et al. Assessment of generative adversarial networks for synthetic anterior segment optical coherence tomography images in closed-angle detection. *Transl Vis Sci Technol.* 2021;10:34. <https://doi.org/10.1167/tvst.10.4.34>.
13. Yildiz E, Arslan AT, Yildiz Tas A, et al. Generative adversarial network based automatic segmentation of corneal subbasal nerves on in vivo confocal microscopy images. *Transl Vis Sci Technol.* 2021;10:33. <https://doi.org/10.1167/tvst.10.6.33>.
14. Zheng C, Xie X, Zhou K, et al. Assessment of generative adversarial networks model for synthetic optical coherence tomography images of retinal disorders. *Transl Vis Sci Technol.* 2020;9:29. <https://doi.org/10.1167/tvst.9.2.29>.
15. Zheng C, Ye H, Yang J, et al. Development and clinical validation of semi-supervised generative adversarial networks for detection of retinal disorders in optical coherence tomography images using small dataset. *Asia Pac J Ophthalmol (Phila).* 2022. <https://doi.org/10.1097/apo.0000000000000498>.
16. Zhou M, Jin K, Wang S, et al. Color retinal image enhancement based on luminosity and contrast adjustment. *IEEE Trans Biomed Eng.* 2018;65:521–527. <https://doi.org/10.1109/tbme.2017.2700627>.
17. Xiong L, Li H, Xu L. An approach to evaluate blurriness in retinal images with vitreous opacity for cataract diagnosis. *J Healthc Eng.* 2017, 5645498. <https://doi.org/10.1155/2017/5645498>.
18. Li J, Xu L. *Romate Ophthalmology.* 2017:96.
19. Zhao H, Yang B, Cao L, Li H, eds. *Data-Driven Enhancement of Blurry Retinal Images via Generative Adversarial Networks.* Cham: Springer; 2019.
20. Miao L, Zhao YQ, Wang XH, et al. *Retinal Vessel Enhancement Based on Multi-Scale Top-Hat Transformation and Histogram Fitting Stretching.* Opt Laser Technol; 2014:56–62.
21. Chaudhuri S, Chatterjee S, Katz N, et al. Detection of blood vessels in retinal images using two-dimensional matched filters. *IEEE Trans Med Imaging.* 1989:263–269. <https://doi.org/10.1109/42.34715>.
22. Su R, Sun C, Zhang C, et al. A new method for linear feature and junction enhancement in 2D images based on morphological operation. *Pattern Recogniti.* 2014:3193–3208.
23. Lin T, Du M, Xu J. The preprocessing of subtraction and the enhancement for biomedical image of retinal blood vessels. *J Biomed Phys Eng.* 2003:56. <https://doi.org/10.3321/j.issn:1001-5515.2003.01.016>.
24. Xiong L, Li H, Xu L. An enhancement method for color retinal images based on image formation model. *Comput Methods Programs Biomed.* 2017;143:137–150. <https://doi.org/10.1016/j.cmpb.2017.02.026>.
25. Zhang J, Li H, Nie Q, et al. A retinal vessel boundary tracking method based on Bayesian theory and multi-scale line detection. *Comput Med Imaging Graph.* 2014;38:517–525. <https://doi.org/10.1016/j.compmedimag.2014.05.010>.